Orientational Phase Transition in a Pyridine Adlayer on Gold(111) in Aqueous Solution Studied by in Situ Infrared Spectroscopy and Scanning Tunneling Microscopy

Wen-Bin Cai, Li-Jun Wan, Hiroyuki Noda, Yuichi Hibino, Kenichi Ataka, and Masatoshi Osawa*

Catalysis Research Center and Graduate School of Environmental Earth Science, Hokkaido University, Sapporo 060-0811, Japan

Received May 27, 1998. In Final Form: October 1, 1998

The orientation and structure of pyridine adsorbed on a highly ordered Au(111) surface from 0.1 M $NaClO_4 + x$ M ($10^{-6} \leq x \leq 10^{-3}$) pyridine aqueous solutions have been investigated as a function of applied potential by in situ surface-enhanced infrared absorption spectroscopy (SEIRAS) and scanning tunneling microscopy (STM). Symmetric in-plane pyridine ring vibrations (A_1 modes) were observed in the SEIRA spectra at potentials positive of about −0.3 V versus SCE, while asymmetric in-plane ring vibrations (B_1 modes) were hardly detected. The symmetric ring-breathing mode showed a blue shift upon adsorption, indicating the adsorption via the N atom. The band intensities were found not to be proportional to the surface concentration (the relative Gibbs surface excess) reported in the literature. On the basis of the surface selection rule in SEIRAS, the results are explained in terms of the potential-dependent reorientation of pyridine. The molecule is flatly adsorbed on the surface at negative potentials, and its molecular plane rises up as the applied potential increases and the surface concentration increases. Flat-lying, tilted, and vertically standing pyridine molecules were observed at different potentials also by STM for the first time.

Introduction

The adsorption of pyridine on metal surfaces, especially on coinage metal (Ag, Au, and Cu) surfaces, has received great interest in both surface science and electrochemistry, since the discovery of surface-enhanced Raman scattering (SERS) for pyridine adsorbed on electrochemically roughened Ag electrodes.[1] Efforts to explain the enormously intense Raman scattering led to an increasing understanding of phenomena associated with the interaction of photons with adsorbates and metal surfaces.[2−5] The variety of adsorption geometries of pyridine depending on surface crystallography and experimental conditions is also of interest. Owing to modern surface analytical techniques, pyridine adstructures have been investigated in detail in ultrahigh vacuum (UHV).[6−13] Four coordination modes of pyridine to metal surfaces have been reported: (1) flat adsorption via π electrons of the aromatic ring; (2) tilted adsorption via both lone-pair electrons of the N atom and π electrons; (3) N-coordinated vertical adsorption; and (4) edge-on adsorption through N and C(2) atoms (as η^2 α-pyridyl by breaking the H−C(2) bond). Flat-oriented pyridine was observed on Ag(111) at low temperature and at low coverages.[6] The flat orientation is rather unstable and is readily converted to a tilted orientation as coverage and/or substrate temperature increases. The tilt angle, the angle between the molecule plane and the surface, was determined to be 45−70°.[6,7] Tilted and almost vertically oriented pyridine molecules were observed also on Au(110),[8] Cu(111),[9] and Cu(110).[10,11] Edge-on adsorption as α-pyridyl species was found on Cu(110),[10] Ni(100),[12] Pt(111),[11,13] and Ru(001)[11] at room temperature.

In contrast to the UHV studies, less is known about the adsorbed geometries of pyridine on metal surfaces in aqueous solutions. Lipkowski et al.[14−21] and Wiekowski et al.[22] quantitatively investigated the pyridine adsorption on polycrystalline and several single-crystal Au surfaces in neutral solutions by chronocoulometry and a radioactive-labeling method. From the thermodynamic data such

* To whom correspondence may be addressed. Fax: +81-11-709-4748. E-mail: osawam@cat.hokudai.ac.jp.

(1) Fleischmann, M.; Hendra, P. J.; McQuillan, A. J. *Chem. Phys. Lett.* **1974**, *26*, 163.
(2) *Surface Enhanced Raman Scattering*; Chang, R. K., Furtak, T. E., Eds.; Plenum: New York, 1982.
(3) Metiu, H. *Prog. Surf. Sci* **1984**, *17*, 153.
(4) Moskovits, M. *Rev. Mod. Phys.* **1985**, *57*, 783.
(5) Otto, A.; Mrozek, I.; Brabhorn, H.; Akemann, W. *J. Phys.: Condes. Matter.* **1992**, *4*, 1143.
(6) Demuth, J. E.; Christmann, K.; Sanda, P. N. *Chem. Phys. Lett.* **1980**, *76*, 201.
(7) Bader, M.; Haase, J.; Frank, K.-H.; Puschmann, A.; Otto, A. *Phys. Rev. Lett.* **1986**, *56*, 1921.
(8) Frank, K. H.; Dudde, R.; Koch, E. E. *Chem. Phys. Lett.* **1986**, *132*, 83.
(9) Bader, M.; Hasse, J.; Frank, K.-H.; Ocal, C.; Puschmann, A. *J. Phys. (Paris)* **1986**, *47*, C8−491.
(10) Bandy, B. J.; Llyoyd, D. R.; Richardson, N. V. *Surf. Sci.* **1987**, *89*, 344.
(11) Bridge, M. E.; Connolly, M.; Lloyd, D. R.; Somers, J.; Jakob, P.; Menzel, D. *Spectrochim. Acta* **1987**, *43A*, 1473.
(12) DiNardo, N. J.; Avouris, Ph.; Demuth, J. E. *J. Chem. Phys.* **1984**, *81*, 2169.
(13) Johnson, A. L.; Muetterties, E. L.; Stohr, J.; Sette, F. *J. Phys. Chem.* **1985**, *89*, 4071.
(14) Stolberg, L.; Richer, J.; Lipkowski, J.; Irish, D. E. *J. Electroanal. Chem.* **1986**, *207*, 213.
(15) Stolberg, L.; Lipkowski, J.; Irish, D. E. *J. Electroanal. Chem.* **1987**, *238*, 333.
(16) Stolberg, L.; Lipkowski, J.; Irish, D. E. *J. Electroanal. Chem.* **1990**, *296*, 171.
(17) Stolberg, L.; Lipkowski, J.; Irish, D. E. *J. Electroanal. Chem.* **1991**, *300*, 563.
(18) Stolberg, L.; Morin, S.; Lipkowski, J.; Irish, D. E. *J. Electroanal. Chem.* **1991**, *307*, 241.
(19) Stolberg, L.; Lipkowski, J.; Irish, D. E. *J. Electroanal. Chem.* **1992**, *322*, 357.
(20) Lipkowski, J.; Stolberg, L.; Morin, S.; Irish, D. E.; Zelenay, P.; Gamboa, M.; Wieckowski, A. *J. Electroanal. Chem.* **1993**, *355*, 147.
(21) Lipkowski, J.; Stolberg, L. In *Adsorption of Molecules at Metal Electrodes*; Lipkowski, J., Ross, P. N., Eds.; VCH: New York, 1992; p 171.
(22) Zelenay, P.; Rice-Jackson, L. M.; Wieckowski, A. *Langmuir* **1990**, *6*, 974.

10.1021/la980617i CCC: $15.00
Published on Web 11/06/1998

as the relative Gibbs surface excess, the Gibbs energy of adsorption, and the electrosorption valency determined by these methods, they proposed that pyridine is adsorbed vertically on (110), (210), and (311) surfaces over the whole double-layer potential region.[16,19,20] At (111), (100), and polycrystalline surfaces, on the other hand, pyridine is adsorbed flat at negative potentials, where the surface concentration is small, and reorients to a vertical orientation as the applied potential shifts positively with an increase in surface concentration.[14,15,18] Unfortunately, such macroscopic measurements do not provide detailed microscopic information on the molecular adsorption.

To determine the adstructure and orientation at the molecular level, physicochemical techniques other than conventional electrochemical techniques are required. Although a number of SERS studies on the pyridine adsorption on Ag, Au, and Cu electrodes have been reported in the literature,[2−5] the interpretation of SER spectra is rather difficult due to the complexity of the enhancing mechanisms of SERS. The so-called oxidation−reduction-cycle pretreatment of the electrode surface in solutions containing halogen ions, which is frequently used to observe strong Raman scattering, makes the situation more complex. Results that support the potential-dependent reorientation proposed from electrochemical measurements have not yet been obtained by SERS. Lipkowski et al.[17,20] compared surface Raman intensities with the surface concentration for pyridine adsorbed on polycrystalline Au, but good correlation was not found between the two measurements at high surface coverage.

Scanning tunneling microscopy (STM) has also been employed by Arvia et al.[23] to characterize the pyridine adlayer on Au(111) in acidic solutions. They demonstrated that pyridine molecules are vertically oriented to the (111) surface and form ordered domains with a (4×4) hexagonal symmetry at potentials more positive than the potential of zero charge (pzc) of the electrode. However, neither flat-lying nor tilted pyridine molecules were observed at negative potentials in their study. To the best of our knowledge, STM observations of pyridine adlayers on Au in neutral solutions have not yet been reported.

Very recently, Ikezawa et al.[24] reported an infrared reflection−absorption spectroscopy (IR-RAS) study on the pyridine adsorption at polycrystalline Au electrodes. Their IR results were not in accordance with the previous chronocoulometry measurements. However, it should be pointed out that the pyridine concentration they used was 10^{-2} M, which is higher than that used in the previous electrochemical measurements (10^{-6} to 10^{-3} M). The high concentration might lead to the formation of a randomly ordered multilayer on Au surfaces.[7]

We report in this paper an in situ IR and STM study on the pyridine adsorption on Au(111) from neutral solutions containing 10^{-6} to 10^{-3} M pyridine. In the IR measurements, we use surface-enhanced IR absorption spectroscopy (SEIRAS)[25] instead of IR-RAS. SEIRAS has a sensitivity over 10 times higher than that of IR-RAS, which allows us to obtain high-quality spectra without interference from the bulk solution. A thin Au film evaporated on Si was used as the working electrode in this measurement. The surface structure and electrochemical properties of the thin film electrode are first characterized by STM, cyclic voltammetry, and differential capacitance measurements. Then IR spectra are compared with the Gibbs surface excess for pyridine adsorbed on Au(111) reported by Lipkowski et al.,[18] from which we will show that the pyridine adlayer exhibits an orientational phase transition with potential change. The orientational phase transition of pyridine is further confirmed by high-resolution STM.

Experimental Section

A Bio-Rad FTS-575C spectrometer equipped with a liquid-N_2-cooled HgCdTe detector was used for SEIRAS measurements and was operated at the resolution 4 cm^{-1}. Spectra of the Au/solution interface were acquired with the so-called Kretschmann attenuated-total-reflection (ATR) configuration (prism/thin metal film/solution geometry), details of which have been described elsewhere.[25−27] Briefly, a 20-nm-thick Au film vacuum-evaporated on a hemicylindrical Si prism was used as the working electrode. Infrared radiation from a ceramic source was focused at the interface by being passed through the prism at the incident angle of 70°, and the totally reflected radiation was detected. Spectra were acquired under potentiostatic or potentiodynamic conditions. All the spectra in this paper are shown in the absorbance units defined as $-\log(I/I_0)$, where I and I_0 represent the intensities of the reflected radiation at the sample and reference potentials, respectively.

The evaporation of Au on the Si prism was performed in a vacuum of 5×10^{-5} Pa from a tungsten basket by thermal heating. The deposition rate was controlled to be 0.01 nm/s by using a quartz microbalance. The surface of the working electrode was cleaned in the test solution before each measurement by repeatedly cycling the potential in the double-layer region of Au to reach a stable cyclic voltammogram.

An EG&G PARC M263 potentiostat was employed to control the electrode potential and to record cyclic voltammograms. In differential capacitance measurements, a small (5 mV rms, 35 Hz) sinusoidal perturbation was superposed onto dc bias voltage, and the real and imaginary components of the impedance were measured with a PARC M5210E lock-in analyzer.

In situ STM observation of the Au/solution interface was carried out with a Digital Instruments Nanoscope E. Tunneling tips were prepared by electrochemical etching of a tungsten wire (0.25 mm in diameter) and were sealed with clear nail polish to minimize the occurrence of Faradaic currents of the tips. All STM images shown in this paper were acquired in the constant-current mode. The (111) facets of an Au single-crystal bead, prepared by melting an Au wire (99.999%), were used for the STM observation. The single-crystal Au bead was annealed in a hydrogen flame for 10 s and then quenched in ultrapure Milli-Q water saturated with hydrogen before use.

All solutions were prepared from ultrapure Milli-Q water. The supporting electrolyte was 0.1 M $NaClO_4$. Super grade chemicals supplied by Wako Pure Chemicals (Tokyo) were used without further purification. The solutions were deaerated with argon prior to the measurements.

The reference electrode used was a saturated calomel electrode (SCE) in electrochemical and infrared measurements and a reversible hydrogen electrode (RHE) in the STM measurements. However, all potentials are reported with respect to SCE.

Results and Discussion

Electrochemistry. Figure 1a shows a typical large-scale STM image of an evaporated Au film electrode observed in 0.1 M $HClO_4$ at 0.1 V. The image shows that the Au thin film consists of particles with an average diameter of about 80 nm. The island morphology of the Au film facilitates the excitation of localized plasmons of the metal. An electric field enhanced through the excitation of plasmons probes the adsorbed molecules, resulting

(23) Andreasen, G.; Vela, M. E.; Salvarezza, R. C.; Arvia, A. J. *Langmuir* **1997**, *13*, 6814.

(24) Ikezawa, Y.; Sawatari, T.; Kitazume, T.; Goto, H.; Toriba, K. *Electrochim. Acta* **1998**, *43*, 3297.

(25) Osawa, M. *Bull. Chem. Soc. Jpn.* **1997**, *70*, 2861 and references therein.

(26) Osawa, M.; Ataka, K.; Yoshii, K.; Yotsuyanagi, T. *J. Electron Spectrosc. Relat. Phenom.* **1993**, *64/65*, 371.

(27) Ataka, K.; Yotsuyanagi, T.; Osawa, M. *J. Phys. Chem.* **1996**, *100*, 10664.

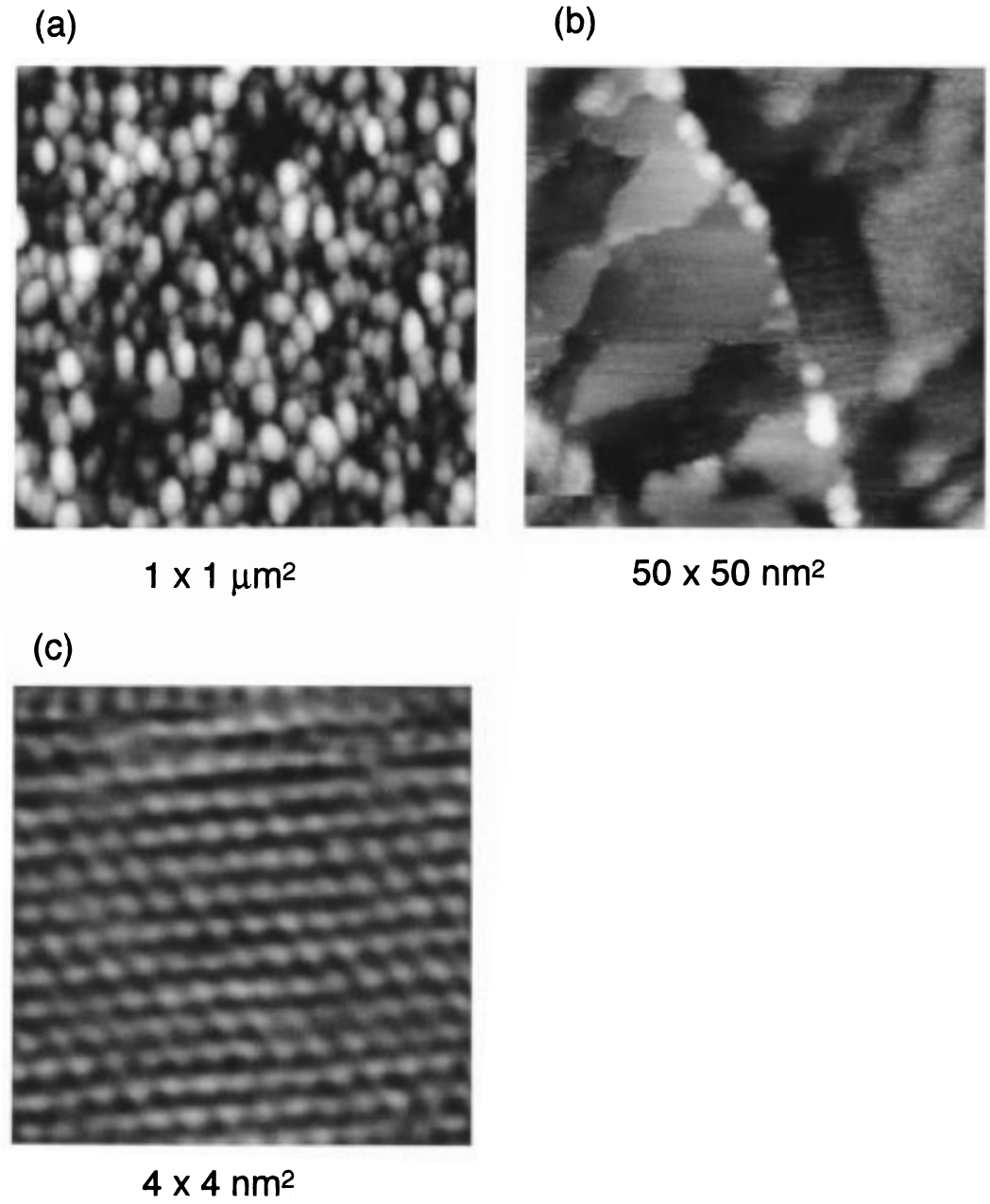

Figure 1. STM images of a thin Au film evaporated on Si observed in 0.1 M $HClO_4$ at 0.1 V versus SCE: (a) a large scale image of the film; (b) an expanded image of a particle showing terrace-step structure; (c) a high-resolution image showing the hexagonal close-packed atomic arrangement characteristic of Au(111).

in the IR absorption enhancement.[25,28] A magnified STM image of a particle (Figure 1b) reveals that the surface of the particle is constructed with terraces and steps. The height of the steps was 0.25 nm, that is, monatomic height. The curved step lines suggest the presence of kinks. Very small Au clusters are also seen to arrange along step lines. A high-resolution STM image of a terrace is shown in Figure 1c, where the well-ordered hexagonal close-packed structure with the interatomic distance 0.29 nm, characteristic of Au(111), is clearly seen. The terrace-step and hexagonal close-packed structures were consistently observed on other particles over the double-layer potential region.

The Au thin film electrode used in IR measurements is preferentially (111) oriented but not an ideal single-crystal electrode, as revealed by STM. Since the pyridine adsorption is very sensitive to the crystallographic orientation of the surface,[14−16,18−21] we investigated first the pyridine adsorption onto this Au thin film electrode by cyclic voltammetry and differential capacitance measurements.

Cyclic voltammograms for the thin film electrode in 0.1 M $NaClO_4$ without and with pyridine (10^{-4} and 10^{-3} M concentration) recorded at the sweep rate 50 mV/s are shown in Figure 2a. In the presence of pyridine, two pairs of peaks appear around 0.2 and −0.5 V. These peaks shift to negative potentials as the bulk pyridine concentration increases.

Shown in Figure 2b are three differential capacitance curves for the Au electrode recorded in the same solutions. The curve in the absence of pyridine displays a diffusion layer minimum at about 0.15 V, which corresponds to the

(28) Osawa, M.; Ataka, K.; Yoshii, K.; Nishikawa, Y. *Appl. Spectrosc.* **1993**, *47*, 1497.

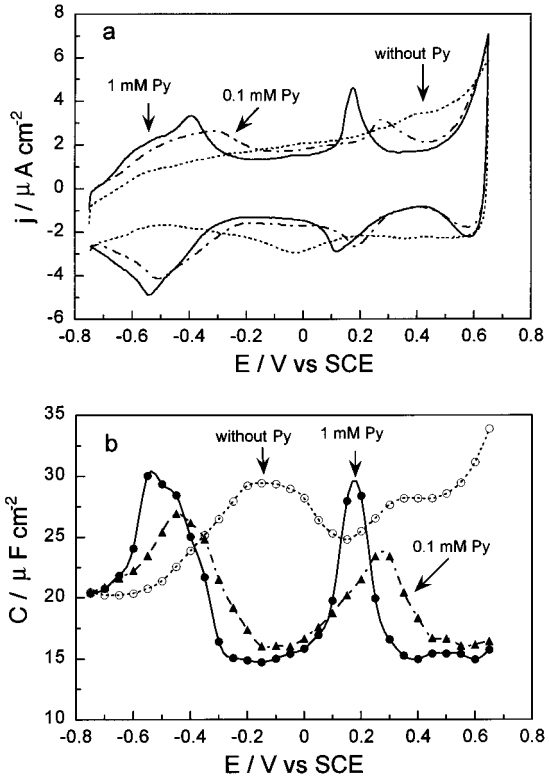

Figure 2. Cyclic voltammograms (a) and differential capacitance plots (b) for an evaporated Au electrode in 0.1 M $NaClO_4$ without and with 1×10^{-4} M and 1×10^{-3} M pyridine (Py).

pzc of the electrode. The pzc of the evaporated Au film electrode is slightly lower than that of Au(111) single-crystal surfaces (0.23[29] or 0.285 V[18]) but is much higher than that of polycrystalline electrodes (−0.04 V[30]). With the addition of pyridine into the solution, two capacitance peaks appear around −0.5 and 0.2 V. The capacitance peaks display a strong dependence on the bulk pyridine concentration, consistent with the voltammograms shown in Figure 2a. The peak seen at the negative potential is typical of the adsorption/desorption of pyridine. The differential capacity curves merge with the curve for the supporting electrolyte around −0.7 V, indicating that the pyridine molecules are desorbed from the Au electrode surface at −0.7 V. The peak at the positive potential has been attributed to a two-dimensional transition in the pyridine adlayer.[18]

The voltammograms and differential capacitance curves for the thin film electrode are similar to those for (111) single-crystal electrodes[18] except for the relatively small intensities of the capacity peaks around 0.2 V for the former electrode. The difference probably arises from surface defects (steps and kinks). The electrochemical measurements ensure the comparison of the IR data taken with the thin film electrode with the chronocoulometric data taken with a (111) single-crystal electrode although the influence of the surface defects must be taken into account.

Infrared Spectra. In this investigation, the IR data for pyridine adsorbed on the highly ordered Au(111) surface are compared with the relative Gibbs surface excess data reported by Lipkowski and co-workers,[18] and special attention is focused on the two-dimensional phase transition signaled in the voltammograms and capacity

(29) Kolb, D. M.; Schneider, J. *Electrochim. Acta* **1986**, *31*, 929.
(30) Clavilier, J.; Huong, C. H. V. *J. Electroanal. Chem.* **1977**, *80*, 101.

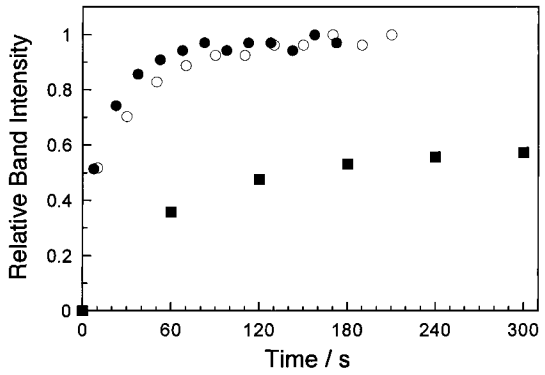

Figure 3. Intensity of the 1599 cm^{-1} band of pyridine adsorbed on a highly ordered Au(111) surface in 0.1 M $NaClO_4$ as a function of time after the potential step from −0.7 to +0.4 V versus SCE for the bulk pyridine concentrations 1×10^{-3} (closed circles), 1×10^{-4} (open circles), and 1×10^{-5} M (closed squares).

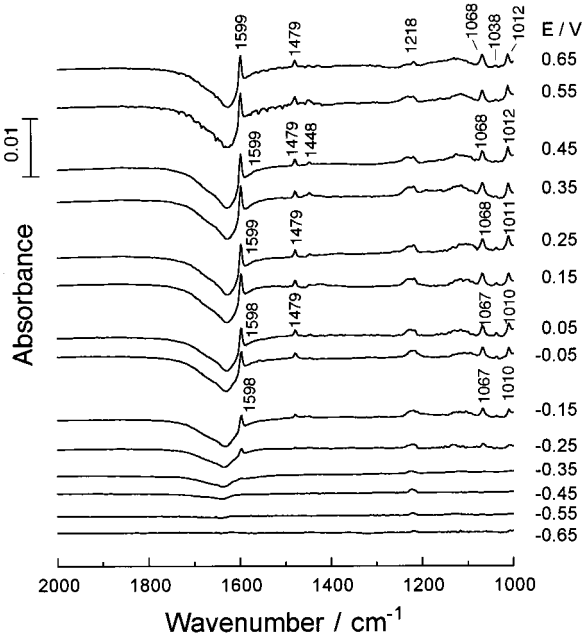

Figure 4. Infrared spectra of pyridine adsorbed on a highly ordered Au(111) surface in 0.1 M $NaClO_4 + 1 \times 10^{-3}$ M pyridine solution as a function of the applied potential. The reference potential was −0.7 V versus SCE.

curves around 0.2 V (Figure 2). The chronocoulometric data were collected after the establishment of adsorption equilibrium in the previous study. Thus infrared measurements also must be carried out under equilibrium conditions for comparison. Lipkowski et al. have shown that it takes several minutes to several tens of minutes for the establishment of adsorption equilibrium, depending on the pyridine concentration.[20] The time required for the equilibrium may be affected also by the structure of the cell and other experimental conditions. To determine the time for adsorption equilibrium under our experimental conditions, we investigated the adsorption dynamics by time-resolved IR spectral measurements. Since both pyridine adsorption and hydrogen evolution can be neglected at −0.7 V (strong hydrogen evolution could cause the Au film to peel off), a spectrum collected at this potential was used as the reference. In Figure 3 the peak intensity of the 1599 cm^{-1} band of pyridine (see Figure 4) is plotted against time after stepping the potential from −0.7 to +0.4 V, where pyridine adsorption is encountered. The intensity increases with time and saturates at about

1, 2, and 5 min for the bulk pyridine concentrations 1×10^{-3}, 1×10^{-4}, and 1×10^{-5} M, respectively. The saturation was observed at about 20 min for the bulk pyridine concentration 1×10^{-6} M (not shown). The band intensities in Figure 3 were normalized to the saturated intensity for the pyridine concentration 1×10^{-3} M. The saturated intensity is constant for the pyridine concentrations 1×10^{-3} and 1×10^{-4} M and is about 0.6 for 1×10^{-5} M. These results are quantitatively well correlated with the surface concentration of pyridine determined by radiochemistry[20] and chronocoulometry,[18] implying that the observed IR bands arise from pyridine molecules adsorbed on the electrode surface. Time-resolved IR measurements also revealed that pyridine molecules are desorbed from the electrode surface within 1 s when the potential is stepped back to −0.7 V.

On the basis of the results described above, a single-beam IR spectrum was collected after holding the potential at a desired value (sample potential) for several minutes (depending on bulk pyridine concentration) to ensure the establishment of adsorption equilibrium. Soon after the collection of the sample spectrum, the reference single-beam spectrum was acquired by stepping the potential to −0.7 V (reference potential) to minimize the spectrometer drift. This procedure was repeated by changing the sample potential. Spectra thus obtained for the pyridine concentration 1×10^{-3} M are shown in Figure 4 as a function of the potential. At potentials negative of −0.35 V, no pyridine bands are observed except for the positive-going broad band at 1230 cm^{-1} and the negative-going band around 1630 cm^{-1}. The former band was observed also with the supporting electrolyte without pyridine. When the deaeration of the solution was insufficient, this band was observed very strongly. Therefore, the 1230 cm^{-1} band may be attributed to some species produced by oxygen reduction. The negative-going band around 1630 cm^{-1} is assigned to the bending mode of water. The negative sign indicates the replacement of water molecules from the electrode surface by the adsorption of pyridine. The doconvolution of the spectra revealed that the water band consists of two components: a sharp band at 1625 cm^{-1} with a half-width of 40 cm^{-1} and a broad band at 1650 cm^{-1} with a half-width of 90 cm^{-1}. The former band is attributed to water molecules directly attaching to the electrode surface.[27,31] The latter band is attributed to water molecules in the overlayers, since its position and width are the same as those for bulk water.

At about −0.3 V, seven bands characteristic of pyridine appear at 1599, 1479, 1448, 1218, 1067, 1038, and 1010 cm^{-1} in the spectral range between 2000 and 1000 cm^{-1}. The spectral range below 1000 cm^{-1} could not be measured due to the strong absorption of the Si prism. These bands grow in intensity as the potential is made more positive. No potential-dependent peak shifts are observed for all these bands within the experimental errors. The same spectral features were observed for lower bulk pyridine concentrations down to 1×10^{-6} M.

The observed peak frequencies for pyridine adsorbed on the Au electrode are listed in Table 1 as well as those for liquid pyridine with relative intensities. The symmetry class and mode number as designated by Corrsin et al.[32] are also indicated. In the notation of symmetry class, the axes are chosen such that the z axis coincides with the C_2 rotation axis and the molecular plane is in the xz plane. The shift of the symmetric ring-breathing (ν_1) mode from 992 cm^{-1} for liquid pyridine (1001 cm^{-1} in aqueous solution) to 1012 cm^{-1} upon adsorption indicates that pyridine is adsorbed on the electrode surface via the N atom on the ring.[2−5] It is noteworthy that the surface spectrum is simpler than the liquid spectrum and is dominated by A_1 modes that have dipole changes along the z axis. The B_1 modes that have dipole changes along the x axis are hardly observed except for the ν_{19b} band, the strongest one in the liquid pyridine spectrum. On the basis of the surface selection rule of SEIRAS that only normal components of dipole changes are IR active,[28] the preferential observation of the A_1 modes is interpreted as the C_2 rotation axis of the molecule being vertical to the surface or tilted with the x axis parallel to the surface. Edge-on adsorption as η^2 α-pyridyl through N and C(2) atoms is exclusively discarded, since such adsorption

Table 1. Frequencies (cm^{-1}) and Assignment of the Observed Bands for Pyridine Adsorbed on Au(111) in 0.1 M $NaClO_4$

mode no.[a]	symmetry[a]	pyridine/Au(111)	liquid pyridine
ν_{8a}	A_1	1599 vs[b]	1580 m
ν_{8b}	B_1		1572 s
ν_{19a}	A_1	1479 m	1482 m
ν_{19b}	B_1	1448 w	1439 vs
ν_{14}	B_1		1375 vw
ν_{9a}, ν_3	A_1, B_1	1218 w	1218 w
ν_{15}	B_1		1148 w
ν_{18b}	B_1		1085 m
ν_{18a}	A_1	1068 m	1068 m
ν_{12}	A_1	1038 w	1029 m
ν_1	A_1	1012 m	992 m

[a] Taken from ref 32. [b] Relative intensity (vs, very strong; s, strong; m, medium; w, weak; vw, very weak).

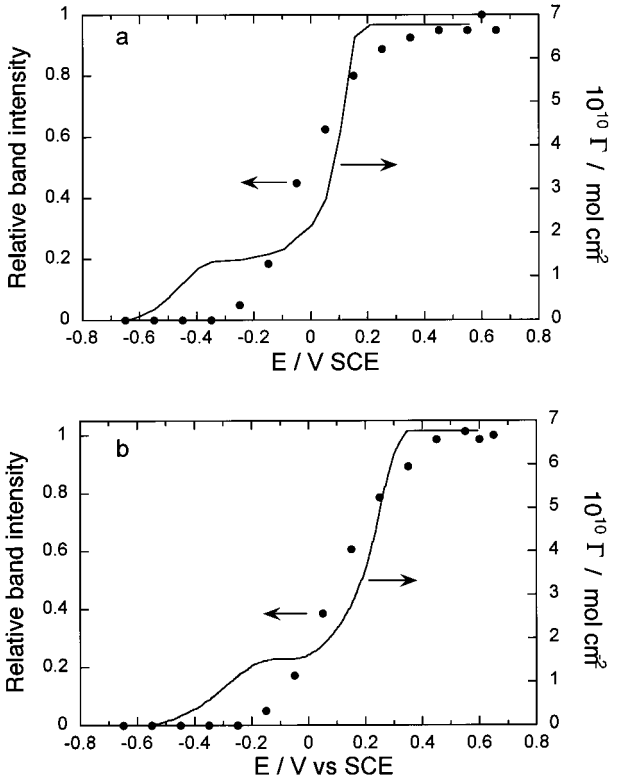

Figure 5. Comparison of the intensity of the 1599 cm^{-1} band of pyridine adsorbed on a highly ordered Au(111) surface in 0.1 M $NaClO_4$ and the Gibbs surface excess (Γ) of pyridine on a single-crystal Au(111) electrode taken from ref 18 as a function of the applied potential.

(31) Ataka, K.; Osawa, M. *Langmuir* **1998**, *14*, 951.
(32) Corrsin, L.; Fax, B. J.; Lord, R. C. *J. Chem. Phys.* **1953**, *21*, 1170.

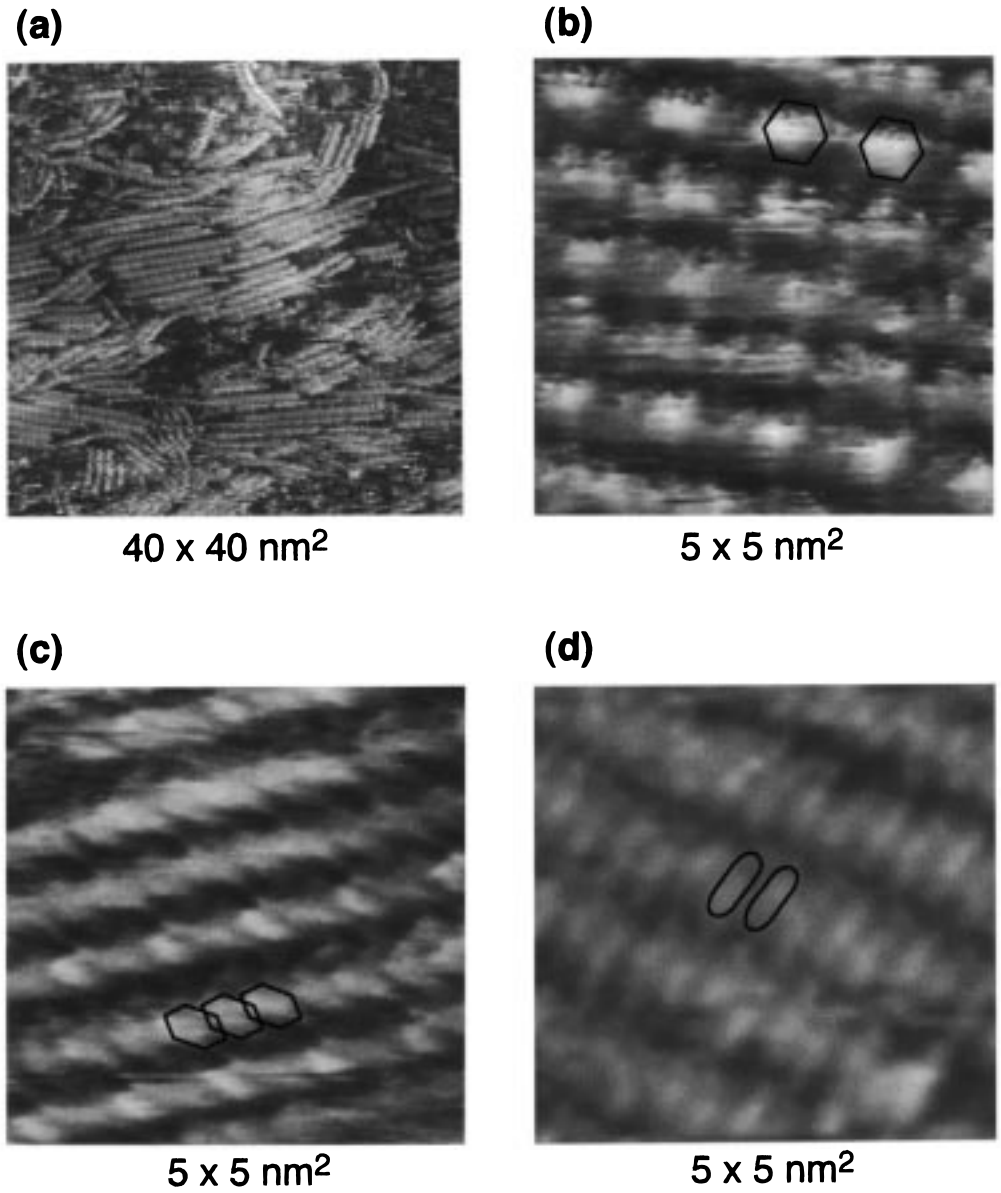

Figure 6. STM images for a pyridine adlayer on an Au(111) electrode in a 0.1 M $NaClO_4 + 1 \times 10^{-4}$ M pyridine solution observed at −0.3 (a and b), 0.1 (c), and 0.3 V (d) versus SCE. The insets show the sizes of flat-lying, tilted, and vertically standing pyridine molecules.

should give the bands corresponding to the B_1 modes of pyridine as strong as those for other modes.[11]

In Figure 5, the integrated intensity of the 1599 cm^{-1} band is compared with the Gibbs surface excess (or surface concentration) data for pyridine adsorbed on a single-crystal Au(111) surface[18] as a function of the applied potential. The other pyridine ring modes showed the same potential dependence (not shown). The profile of the IR intensity versus potential curves is similar to that of the surface concentration versus potential curves, but the IR intensity is not perfectly proportional to the surface concentration, as is seen from the figure. Although pyridine is definitely adsorbed on the surface at potentials positive of −0.7 V (Figure 2), the pyridine bands are observed only at potentials more positive than −0.3 and −0.2 V for the pyridine concentrations 1×10^{-3} M (a) and 1×10^{-4} M (b), respectively. The band intensity starts to increase in the potential range where the surface concentration is almost constant (between −0.3 and −0.1 V for 1×10^{-3} M and between −0.2 and 0 V for 1×10^{-4} M) and continues to increase up to about 0.4 V although the surface concentration saturates at 0.2−0.3 V.

It has been reported that pyridine has a tendency to segregate at defect sites or high index facets, leaving the low-index adsorption sites unoccupied.[20,21] However, the observed discrepancy between the IR and surface concentration data cannot be attributed to the adsorption at the defect sites existing on the electrode surface used in the IR measurements because pyridine adsorption at defect sites is encountered at more negative potentials than −0.2 V. For example, the Gibbs surface excess saturates at about −0.5 V at stepped Au(210) and at −0.2 V at kinked Au(311) for the bulk pyridine concentration 1×10^{-4} M.[20,21] The IR data are not correlated also with the surface excess data for Au(100), (110), and polycrystal surfaces.[20,21] Therefore, it is believed that the absorption by pyridine molecules adsorbed on (111) terraces dominates the IR spectra shown in Figure 4.

It is important to note that the band intensity greatly depends on the molecular orientation and is not necessarily

proportional to the surface concentration. The electric field, $\vec{E}$, that probes the adsorbed molecules is polarized along the surface normal at any points of metal particles.[25,26,28] If the dipole change of a vibrational mode, $d\vec{\mu}/dQ$, is inclined by θ from the surface normal, then the band intensity is represented as

$$I \propto C_{surf}|\vec{E}\cdot\frac{d\vec{\mu}}{dQ}|^2 = C_{surf}\cos^2\theta|\vec{E}|^2|\frac{d\vec{\mu}}{dQ}|^2$$

where C_{surf} represents the surface concentration of the molecule. Dipole−dipole coupling between adsorbed molecules not taken into account in this equation may also affect the intensity. The missing of the in-plane pyridine ring modes at potentials negative of −0.3 V clearly indicates that the molecules are lying nearly flat ($\theta \approx 90°$) in this potential region. In turn, the appearance and growth of the pyridine bands at more positive potentials indicates that the molecular plane is not parallel to the surface. Unfortunately, the tilt angle of the pyridine ring plane ($= 90° - \theta$) could not be determined quantitatively in the present IR study because the spectral measurements were limited only to the in-plane ring vibration region (above 1000 cm^{-1}) due to the strong absorption of the Si prism used. Nevertheless, the increase in band intensity in the potential ranges where the surface concentration of pyridine is constant (between −0.3 and −0.1 V and above 0.2 V for the bulk pyridine concentration 1×10^{-3} M) suggests that the tilt angle increases as the potential increases.

STM Observation. To confirm the orientational phase transition of pyridine deduced from the IR measurements, we further investigated the pyridine adlayer on Au(111) by STM that is capable of providing real space insight into the molecular structure. Figure 6a shows a typical STM image of a pyridine adlayer on a Au(111) terrace in 0.1 M $NaClO_4$ solution containing 1×10^{-4} M pyridine observed at −0.3 V, where pyridine molecules are expected to orient flat. Both ordered and disordered domains are seen, as in the case in acidic solutions.[23] Molecular rows in the ordered domains were found to extend along the Au(111)-[121] (or $\sqrt{3}$) direction relative to the underlying Au(111) lattice. Similar STM images in which ordered and disordered domains coexist were observed at potentials more positive than −0.3 V and at higher pyridine concentrations. However, careful observations revealed that the molecular arrangement in the domains is strongly dependent on the applied potential, as described below.

A high-resolution STM image of an ordered domain acquired at −0.3 V is shown in Figure 6b. Blobs with a dimension of about 0.6 nm are seen to be arranged along the $\sqrt{3}$ direction. Since these blobs disappeared and the hexagonal close-packed pattern characteristic of Au(111) appeared when the potential was shifted to −0.7 V, these blobs are attributed to adsorbed pyridine molecules. Although the molecular structure is not clearly imaged probably due to the weak chemisorption of pyridine on Au(111),[18] the size of the blobs corresponds to pyridine molecules lying flat on the surface.

Figure 6c shows an STM image of an ordered pyridine domain acquired at 0.1 V. This image appears as a set of hexagonal-shaped "dominoes" fallen along the $\sqrt{3}$ direction, and the "dominoes" appear to be partly piled up, as schematically illustrated in the figure. The molecular image resembles the adstructure for tilted pyridine molecules on Ag(111) adsorbed through the N atom and π electron of the ring determined by EELS and UPS in UHV.[6] Thus we attribute the hexagonal-shaped "dominoes" to tilted pyridine molecules adsorbed on the Au(111) surface. The adlayer is roughly defined as a $3 \times \sqrt{3}$ structure. The number of pyridine rings observed in this image is roughly twice that observed in Figure 6b, corresponding to the increase in the relative Gibbs surface excess (see Figure 4b, solid line) although quantitative comparison is difficult due to the presence of disordered domains.

When the potential is shifted to 0.3 V, the STM image shown in Figure 6d was observed. In this image the vertically standing pyridine molecules are seen to stack into polymeric chains such as rolls of "coins" with the intermolecular distance of about 0.5 nm along the $\sqrt{3}$ direction. The thickness of each "coin" is around 0.35 nm, close to that of the aromatic ring (0.34 nm[33]). Although Arvia and co-workers reported that the vertically adsorbed pyridine molecules yield a well-ordered (4×4) hexagonal lattice in 0.1 M $HClO_4$ at potentials more positive than the pzc,[23] such an adstructure was not observed in the neutral solution.

Conclusion

ATR-SEIRAS allowed us to obtain high-quality IR spectra of pyridine adsorbed on a highly ordered Au(111) surface from 0.1 M $NaClO_4$ aqueous solutions containing 10^{-6} to 10^{-3} M pyridine without interference from the bulk solution. Although the electrode used was an island film consisting of Au particles of 80 nm in average diameter, STM observation and electrochemical measurements revealed that the (111) planes preferentially appeared on the particle surfaces. The electrochemical behavior of this electrode was nearly the same as that of single-crystal Au(111) surfaces, which allowed a comparison of the IR data with previously reported chronocoulometric data for a (111) single-crystal electrode. Pyridine molecules are adsorbed on the electrode surface at potentials more positive than −0.6 V, but symmetric in-plane ring modes of adsorbed pyridine were observed only at potentials more positive than −0.3 V and grew in intensity as the potential increased. Asymmetric in-plane modes were hardly observed in the whole double-layer potential region. The band intensities were not proportional to the Gibbs surface excess. On the basis of the surface selection rule in SEIRA, these results were interpreted as that pyridine is adsorbed flat on the surface at negative potentials and the molecular plane gradually rises up as the potential increases, which is in accordance with the predictions made previously from electrochemical measurements.

The molecular orientation was further investigated by STM. Pyridine adsorption on Au(111) facets yielded both ordered and disordered domains. The flat-lying, tilted, and vertically standing pyridine molecules were observed in the ordered domains at different potentials in accordance with the IR measurements.

Acknowledgment. This work was supported by a Grant-in-Aid for Scientific Research on Priority Area of "Electrochemistry of Ordered Interfaces" (No. 09237101) and of "Near-Field Nano-optics" (No. 09241201), for Scientific Research (B) (No. 08454171), and for COE Research from the Ministry of Education, Science, Sports and Culture of Japan.

LA980617I

(33) Pauling, L. C. *The Nature of the Chemical Bond*, 3rd ed.; Cornel University Press: New York, 1960.